# Characteristic difference between ITO/ZrCu and ITO/Ag bi-layer films as transparent electrodes deposited on PET substrate

C.J. Lee[a], H.K. Lin[b,*], S.Y. Sun[a], J.C. Huang[a]

[a] Department of Materials and Optoelectronic Science, Center for Nanoscience and Nanotechnology, National Sun Yat-Sen University, Kaohsiung 804, Taiwan, ROC
[b] Laser Application Technology Center/Industrial Technology Research Institute South (ITRI South), 8, Gongyan Rd., Liujia Shiang, Tainan County 734, Taiwan, ROC

## ARTICLE INFO

## ABSTRACT

The metallic-glass film of ZrCu layer deposited by co-sputtering was utilized as the metallic layer in the bi-layer structure transparent conductive electrode of ITO/ZrCu (IZC) deposited on the PET substrate using magnetron sputtering at room temperature. In addition, the pure Ag metal layer was applied in the same structure of transparent conductive film, ITO/Ag, in comparison with the IZC film. The ZrCu layer could form a continuous and smooth film in thickness lower than 6 nm, compared with the island structure of pure Ag layer of the same thickness. The 30 nm ITO/3 nm ZrCu films could show the optical transmittance of 73% at 550 nm wavelength. The 30 nm ITO/12 nm ZrCu films could show the better sheet resistance of 20 Ω/sq, but it was still worse than that of the ITO/Ag films. It was suggested that an alloy system with lower resistivity and negative mixing heat between atoms might be another way to form a continuous layer in thickness lower than 6 nm for metal film.

## 1. Introduction

Transparent conductors are materials, usually in thin-film form, which simultaneously combine low resistance and high transparency. Transparent conductor films deposited on substrates are used in a variety of applications such as organic light-emitting devices, solar cells and flat panel displays (FPD) [1–3]. At present, indium tin oxide (ITO) thin films as transparent conductive electrodes are widely used in different applications because of their low electrical resistance and high transmittance in the visible range of the spectrum [4,5]. For the goal of getting better sheet resistance (<100 Ω/sq), the thickness of ITO thin film must reach to 100 nm [6,7], but this would lead to a disadvantage owing to the high cost of indium. In order to decrease the use of ITO materials by reducing the thickness of ITO film, the transparent conductor films in thickness lower than 100 nm with the sandwich structure of ITO–metal layer–ITO have been verified the performance of good conductivity and transparency in visible light range [3,8–11] due to higher carrier concentration in the middle layer of metal film [11]. The metal materials of middle layer were generally silver or copper, some of highly conductive metals, and the optimal thickness of middle layer was about 8–12 nm [8,11] to couple the good transmittance in visible light and higher conductivity. The thinner metal film (<8 nm) would exhibit worse conductivity due to the discontin-

uous film of island structure; however, the thicker and continuous metal film would result in the high reflectivity to lower the entire transmittance in visible spectrum because of the continuous film structure and higher plasma frequency of metal materials. The same sandwich structure could also get the similar optical and electrical performance in other transparent conducting oxide, for example, ZnO–Ag–ZnO [12] or ZnS–Ag–ZnS [13].

The metallic glass was a metallic material without the long-range order of crystalline structure, displaying an amorphous structure. In the traditional process, such as the rapid quenching method from liquid to solid state, Inoue [14] has proposed some empirical rules, namely, multicomponent systems consisting of more than three elements, significant difference in atomic size ratio above 12%, and negative heats of mixing among the constituent elements. Systems satisfying these rules could have the chance to be fabricated into bulk metallic glasses (BMGs). Nevertheless, the processing and material composition windows for fabricating the metallic glasses would be broader if they are prepared from the vapor to solid state. For example, sputtering or evaporation deposition can be proceeded at much higher cooling rates ($10^{10}$ to $10^{12}$ K/s) than of rapid solidification ($10^3$ to $10^8$ K/s). These metallic-glass films could exhibit better surface roughness [15] and other unique properties as compared with the pure metallic films [16,17]. The superior surface roughness of metallic-glass films may be due to high nucleation rate during deposition even if at the early stage of film growth. Therefore, this high nucleation rate of metallic-glass films would have the chance to form the continuous film with the thinner metal layer in the sandwich

* Corresponding author. Tel.: +886 6 6939086; fax: +886 6 6939056.
*E-mail address:* hsuankai@msn.com (H.K. Lin).

**Table 1**
Detailed parameters of film depositions.

| | ITO film | Co-sputter ZrCu film | | Ag film |
| --- | --- | --- | --- | --- |
| | ITO target | Zr target | Cu target | Ag target |
| Base pressure | $9 \times 10^{-6}$ Torr | $9 \times 10^{-6}$ Torr | $9 \times 10^{-6}$ Torr | $9 \times 10^{-6}$ Torr |
| Working pressure | $8 \times 10^{-3}$ Torr | $4 \times 10^{-3}$ Torr | $4 \times 10^{-3}$ Torr | $4 \times 10^{-3}$ Torr |
| Ar flow rate | 50 sccm | 30 sccm | 30 sccm | 30 sccm |
| Discharge power | 150 W | 140 W | 84 W | 80 W |

structure or bi-layer structure of transparent conductor films. This transparent conductor films with thinner metal layer could have an opportunity to perform the good transparency and conductivity, simultaneously.

To date, various studies have documented the characteristics of ITO multilayer with pure metal. However, the studies of metallic-glass films substituting for pure metal are still seldom addressed. Hence, the bi-layer structures, consisting of a metallic-glass film of ZrCu alloy and an outer layer of ITO, were chosen to prepare the transparent conductive film deposited on a flexible substrate of polyethylene terephthalate (PET). We also investigate the influence of metallic-glass film on optoelectronic properties of this transparent conductive electrode, and compare the difference with the same structure films when pure Ag film is replaced by the ZrCu film.

## 2. Experimental method

The bi-layer structure of ITO/ZrCu films (termed IZC films) and ITO/Ag films (termed IA films) were deposited by the sputtering process onto the PET substrate (DuPontTeijin ST504). The transmittance of PET is 88% at wavelength of 550 nm and the thickness of 125 μm. The ITO target with composition of 90 wt.% $In_2O_3$ and 10 wt.% $SnO_2$, and the metallic-glass film of ZrCu alloy was deposited by the co-sputtering method. All targets are measuring 4 in. in diameter and the deposition conditions are listed in Table 1. The thickness of the ITO layer was fixed at 30 nm and that of the metallic films was varied from 3 to 12 nm. The morphology and components ratio of films were examined by scanning electron microscopy (SEM) with energy dispersive spectrometry (EDS). The crystalline structures of films were also examined by grazing incidence in-plane X-ray diffraction (GIXD). The sheet resistance was measured using a 4-point probe technique. Optical transmittance and reflectivity were measured in the range of 200–1000 nm by UV–vis–IR spectrophotometer (N&K analyzer 1280).

## 3. Results and discussions

In order to conveniently observe the film morphology of initial growth, the ZrCu and pure Ag layers were first deposited on the Si-wafer substrate, since the non-conductivity of PET substrate is unfavorable for SEM observation. Fig. 1 shows the surface morphology of two films in 3 nm and 6 nm thickness. The ZrCu layers 3 nm or 6 nm in thickness were uniformly and smoothly deposited on the Si substrate, suggesting that this ZrCu thin layer was a continuous film; however, the 6 nm Ag film still appeared the discontinuous island structure, showing the trace of initially lateral growth. The component ratio of ZrCu layer was identified by SEM–EDS to be $Zr_{54}Cu_{46}$. The XRD pattern of the ZrCu layers deposited on Si wafer is presented in Fig. 2, and the diffraction result appears one broadening and diffuse peak, typical for the amorphous structure. In addition, the deposited ITO layer is also the amorphous structure. The pure Ag layer deposited on Si wafer is the crystalline phase and appears the preferred orientation of (1 1 1) peak, as shown in Fig. 2.

As the pure Ag atoms deposited on a "perfect" surface, the embryo radius depended on the surface tension, activation energy of desorption and depositional temperatures, and it could be thought as homogeneous nucleation. Apart from the above factories affecting the embryo radius, the negative heat of mixing between Zr and Cu atoms ($\Delta H_{mix} \sim -23$ kJ mol$^{-1}$) would increase the attractive force during the deposition of ZrCu layer by co-sputtering. This attractive force could lead to chemical cluster sites and promote the amorphous ZrCu layer to be heterogeneously nucleated. This heterogeneous nucleation of ZrCu layer deposited at room temperature would show a smaller radius of embryo and a higher density of embryo number than the homogeneous nucleation of pure Ag layer; therefore, the ZrCu layer would readily show the continuous and smooth film even if at 3 nm thickness.

The optical transmittance and reflectivity of IZC and IA films on the PET substrate are shown in Fig. 3, as a function of metallic thickness. The transmittance of the pure single-layer ITO film was about 83% in the visible wavelength of 550 nm. The IZC films showed the similarly transparent trend with pure ITO film in the measured spectrum, but the transmittance declined with increasing amorphous ZrCu layer thickness, as shown in Fig. 3(a). The transmittance of IZC films with 3 nm thickness of ZrCu layer was 73% at 550 nm wavelength and it is relatively fixed from 500 to 1000 nm wavelengths. However, for IA films, the maximum transmittance of IA films with pure Ag film 6 nm in thickness was about 73% at wavelength of 480–540 nm, and the transmittance gradually declined to 54% upon further increase of wavelength. The rate of decline in the transmittance upon the wavelength of 500 nm was severer in the 9 nm Ag film than that of the 6 nm Ag one. As for the optical reflectivity, the reflectivity of the IZC films with ZrCu films of varying thicknesses maintained within the ratio of 10–23%. By contrast, the reflectivity of IA films at wavelengths greater than 550 nm gradually increased with increasing Ag thickness.

Taking account of the conservation of energy, the incident energy into the transparent substance could be expressed as

$$\text{Incident power} = 1 = T + R + L, \tag{1}$$

where $T$ is defined as the ratio of the transparent power to the incident power, $R$ is the ratio of reflective power to the incident power, $L$ is energy loss due to absorption or scattering power. Table 2 lists the transparent, reflective and energy loss ratio for all transparent films at 550, 750 and 950 nm wavelength. For IZC films, the energy loss, $L$, of incident energy was directly proportional to the thickness of amorphous ZrCu layers; nevertheless, the energy loss in IA films was indirectly proportional to the crystalline Ag film thickness. Based on the observation of Fig. 1, the thickness of Ag layer lower than 6 nm was still in the island structure stage of film growth, and this discontinuous film of island structure would easily lead to the light scattering. As the Ag layer deposited to 9 nm, it might form a continuous film to gradually reflect the incident light especially at longer wavelengths [11]. It was suggested that the energy loss of IA films might be dominated by the scattering of discontinuous Ag layer. In contrast to the island structure in Ag layer with a thickness lower than 9 nm, the ZrCu layer deposited by co-sputtering was a continuous film even with a thickness of only 3 nm. This continuous and smooth metal layer without the
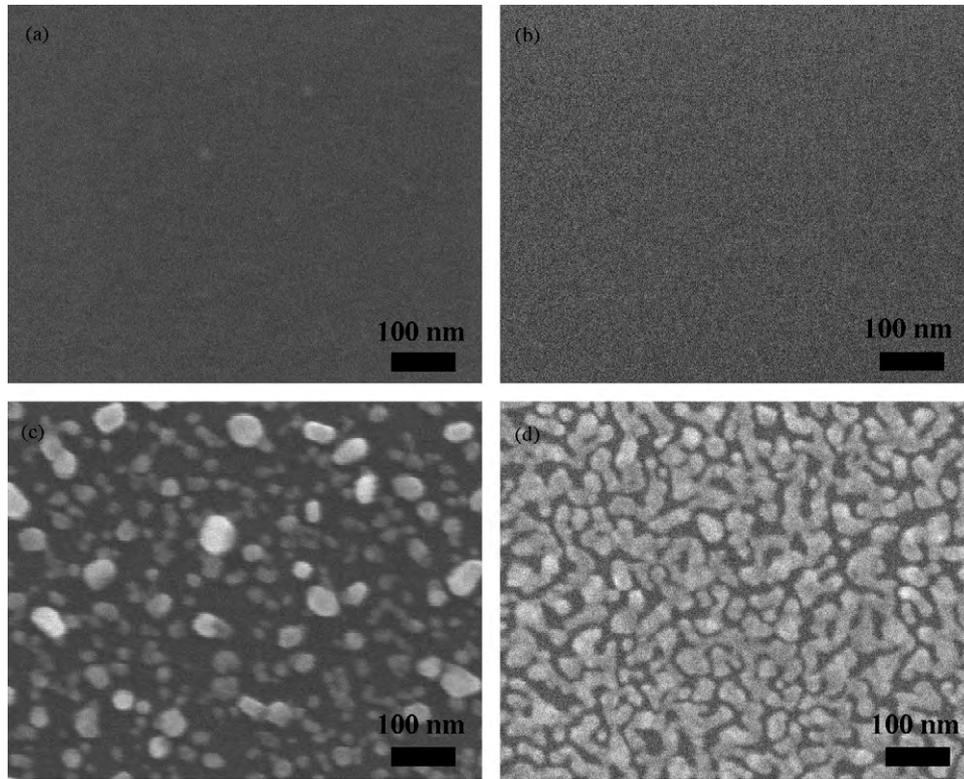
**Fig. 1.** The surface morphology of thin metal layer deposited on Si wafer: (a) 3 nm ZrCu layer, (b) 6 nm ZrCu layer, (c) 3 nm Ag layer and (d) 6 nm Ag layer.
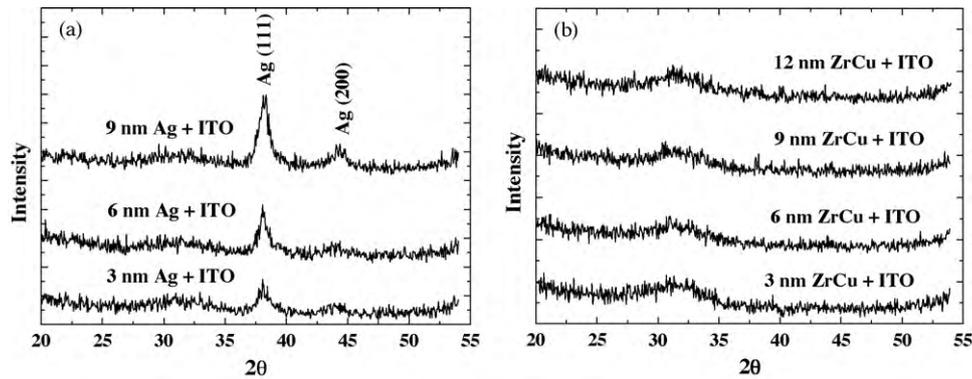


**Fig. 2.** X-ray diffraction for the (a) ITO/Ag and (b) ITO/ZrCu bi-layer deposited on the Si wafer.

island structure would successfully reduce the scattering of incident light. Based on the energy loss directly proportional to the thickness increase of ZuCu layer, it is suggested that the absorption of ZrCu layer to incident light dominates this energy loss.

Fig. 4 shows the sheet resistance of IZC and IA films. Based on assumption of the parallel combination of the two layers, the resistivity of amorphous ZrCu and crystalline Ag layers could be calculated as:

$$\rho_{metal} = d_{metal} \left( \frac{1}{R_{sq}} - \frac{d_{ITO}}{\rho_{ITO}} \right)^{-1},$$

**Table 2**
Transmittance and reflectivity at 550, 750 and 950 nm light wavelengths for the IZC and IA films.

|  | ITO, 30 nm | IZC, 30/3 nm | IZC, 30/6 nm | IZC, 30/9 nm | IZC, 30/12 nm | IA, 30/3 nm | IA, 30/6 nm | IA, 30/9 nm |
|---|---|---|---|---|---|---|---|---|
| 550 nm | 82.4% (10.2%) ⟨7.4%⟩ | 72.5% (13.1%) ⟨14.4%⟩ | 62.6% (14.7%) ⟨22.7%⟩ | 53.3% (13.0%) ⟨33.7%⟩ | 45.4% (14.1%) ⟨39.5%⟩ | 59.2% (9.9%) ⟨30.9%⟩ | 72.2% (5.1%) ⟨22.7%⟩ | 57.2% (27.0%) ⟨15.8%⟩ |
| 750 nm | 86.0% (8.5%) ⟨5.5%⟩ | 75.5% (10.9%) ⟨13.6%⟩ | 65.1% (12.7%) ⟨22.2%⟩ | 55.3% (12.9%) ⟨31.8%⟩ | 45.4% (16.0%) ⟨38.6%⟩ | 57.4% (12.1%) ⟨30.5%⟩ | 62.9% (15.2%) ⟨21.9%⟩ | 31.7% (55.1%) ⟨13.2%⟩ |
| 950 nm | 87.8% (7.5%) ⟨4.7%⟩ | 77.3% (9.7%) ⟨13.0%⟩ | 67.1% (11.0%) ⟨21.9%⟩ | 57.3% (12.4%) ⟨30.3%⟩ | 45.7% (16.5%) ⟨37.8%⟩ | 56.3% (13.3%) ⟨28.4%⟩ | 53.9% (26.2%) ⟨19.9%⟩ | 20.0% (69.0%) ⟨11.0%⟩ |

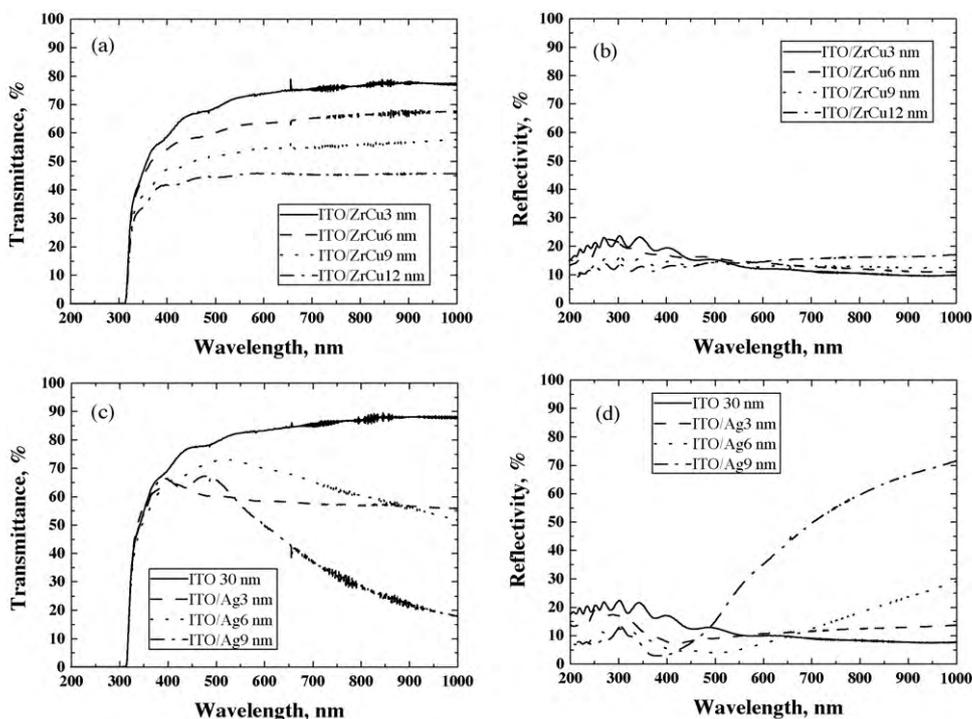PS: ( ) represents the reflectivity, ⟨ ⟩ represents the light loss.

**Fig. 3.** Optical transmittance and reflectivity spectra for (a) transmittance of ITO/ZrCu bi-layer, (b) reflectivity of ITO/ZrCu bi-layer, (c) transmittance of ITO/Ag bi-layer and 30 nm ITO, and (d) reflectivity of ITO/Ag bi-layer and 30 nm ITO.

where $\rho$ is the resistivity of metal or ITO layers, $d$ is the thickness of metal or ITO layers and $R_{sq}$ is the sheet resistance of IZC or IA films, and these results are also shown in Fig. 4. The sheet resistance of ITO in 30 nm thickness was 950 $\Omega$/sq. The sheet resistance of IZC films varied from 623 to 20 $\Omega$/sq with increasing thickness of ZrCu layer from 3 to 12 nm, and appears to be worse than that of IA films varying from 42 to 0.7 $\Omega$/sq with increasing thickness of Ag layer from 3 to 9 nm. The resistivity of Ag layer is seen to be lowered from 13.2 to 0.6 $\mu\Omega$ cm with increasing Ag layer thickness from 3 to 9 nm. The variation of Ag resistivity could be interpreted from the viewpoint of electron transmission path. The electron transmission would be scattered at the Ag and ITO interface due to the island structure of Ag layer, especially for thicknesses lower than 6 nm. As the thickness of Ag layer grew to 9 nm, it would develop a continuous film to form an unobstructed path for electron transmission [11]. In contrast with the severe variation on resistivity of Ag layer, that of ZrCu layer nearly maintained at the region of 150 $\mu\Omega$ cm after the thickness of ZrCu layer is greater than 3 nm.

The resistivity of the ZrCu thin-film layer ($Zr_{54}Cu_{46}$) was close to the 180 $\mu\Omega$ cm of amorphous $Zr_{43}Cu_{57}$ alloy [18]. The result showed that the ZrCu layer could nearly reach the theoretical resistivity at layer thickness of 6 nm as a result of the formation of continuous film at 3–6 nm thickness by Zr and Cu co-sputtering. Although the ZrCu layer could form a continuous film in thinner thickness of 3–6 nm by the negative heat of mixing between the Zr and Cu atoms, inducing a large amount of nucleation sites, the amorphous structure of ZrCu layer readily resulted in the electron scattering during carrier transmission to show the lower conductivity than that of the crystalline metal pure Ag. Therefore, introducing other alloy systems with lower resistivity and lower $T_g$ (glass transition temperature), for example $Mg_{80}Cu_{20}$ (with a much lower resistivity of 52 $\mu\Omega$ cm and lower $T_g$ of 130–140 $^\circ$C) or others, could form a continuous layer in thickness lower than 6 nm to perform the better transmittance. And the subsequent surface annealing to induce the crystallization would be suggested improving the conductivity owing to eliminating the electron scattering of the amorphous structure. This metallic-glass layer by co-sputtering deposition differing from the pure metal layer, which need the thicker layer than 9 nm to form a continuous film, would be an another choice.
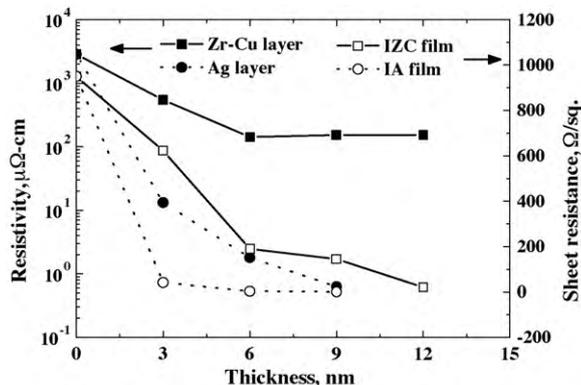
## 4. Conclusions

ITO/ZrCu (IZC) and ITO/Ag (IA) bi-layer films were deposited on PET substrate using magnetron sputtering at room temperature. The amorphous structure of ZrCu layer deposited by co-sputtering could form a continuous film in thickness thinner than 6 nm by the large amount of nucleation sites due to the negative heat of mixing between the Zr and Cu atoms. IZC (ITO 30 nm/ZrCu 3 nm) films could show the optical transmittance of 73% at 550 nm wavelength. With increasing the thickness of metal layer, the reflectivity of IZC films did not show the same characteristic of higher reflectivity of IA films at wavelengths longer than 550 nm. The IZC (ITO 30 nm/ZrCu 12 nm) films could show the better sheet resistance of 20 $\Omega$/sq, but it was still worse than that of the IA films. It was suggested that



**Fig. 4.** Resistivity of ZrCu and Ag layers, and sheet resistance of IZC and IA films as a function of metal layer thickness.

an alloy system with lower resistivity and negative mixing heat between atoms might be another way to form a continuous layer in thickness lower than 6 nm for metal film for transparent conductor designs.

## Acknowledgements

## References

[1] H. Kim, C.M. Gilmore, A. Pique, J.S. Horwitz, H. Mattoussi, H. Murata, Z.H. Kafafi, D.B. Chrisey, Journal of Applied Physics 86 (1999) 6451–6461.
[2] A. Kloppel, B. Meyer, J. Trube, Thin Solid Films 392 (2001) 311–314.
[3] C. Guillen, J. Herrero, Solar Energy Materials and Solar Cells 92 (2008) 938–941.
[4] C.G. Granqvist, A. Hultaker, Thin Solid Films 411 (2002) 1–5.
[5] O.J. Gregory, Q. Luo, E.E. Crisman, Thin Solid Films 406 (2002) 286–293.
[6] C. Guillen, J. Herrero, Thin Solid Films 480–481 (2005) 129–132.
[7] J. Lee, H. Jung, J. Lee, D. Lim, K. Yang, J. Yi, W.-C. Song, Thin Solid Films 516 (2008) 1634–1639.
[8] M. Bender, W. Seelig, C. Daube, H. Frankenberger, B. Ocker, J. Stollenwerk, Thin Solid Films 326 (1998) 67–71.
[9] K.H. Choi, J.Y. Kim, Y.S. Lee, H.J. Kim, Thin Solid Films 341 (1999) 152–155.
[10] A. Kloppel, W. Kriegseis, B.K. Meyer, A. Scharmann, C. Daube, J. Stollenwerk, J. Trube, Thin Solid Films 365 (2000) 139–146.
[11] A. Indluru, T.L. Alford, Journal of Applied Physics 105 (2009) 123528.
[12] D.R. Sahu, S.Y. Lin, J.L. Huang, Applied Surface Science 252 (2006) 7509–7514.
[13] X.J. Liu, X. Cai, J.F. Mao, C.Y. Jin, Applied Surface Science 183 (2001) 103–110.
[14] A. Inoue, Materials Science and Engineering A—Structural Materials Properties Microstructure and Processing 304 (2001) 1–10.
[15] C.W. Chu, J.S.C. Jang, G.J. Chen, S.M. Chiu, Surface & Coatings Technology 202 (2008) 5564–5566.
[16] Y.D. Liu, S. Hata, K. Wada, A. Shimokohbe, Japanese Journal of Applied Physics Part 1-Regular Papers Short Notes & Review Papers 40 (2001) 5382–5388.
[17] J.P. Chu, C.T. Liu, T. Mahalingam, S.F. Wang, M.J. O'Keefe, B. Johnson, C.H. Kuo, Physical Review B 69 (2004) 113410.
[18] J.S. Dugdale, The Electrical Properties of Disordered Metals, Cambridge University Press, New York, 1995.